Immunopathologia Persa
http immunopathol.com
DOI:10.34172/ipp.2025.43824

Investigating the anti-proliferative effects of benzenesulfonamide derivatives on human lung cancer cells; an in-vitro analysis study

Hiba Nabil Miran[1*], Ghaith Ali Jasim[2], Tareq Hafdhi Abidtawfeeq[3]

[1]College of Pharmacy, Mustansiriyah University, Baghdad, Iraq
[2]College of Health and Medical Techniques, Al-Bayan University, College of Pharmacy, Mustansiriyah University, Baghdad, Iraq
[3]University of Al-Farahidi, Baghdad, Iraq

***Correspondence to**
Hiba Nabil Miran,
Email: heba_nabil@uomustansiriyah.edu.iq

Received 24 Oct. 2024
Revised: 22 Jan. 2025
Accepted 2 Feb. 2025
ePublished 4 Mar. 2025

Keywords: Lung neoplasms, Benzenesulfonamide, Cell proliferation, Reactive oxygen species, Cytotoxicity, Antioxidant

Abstract

Introduction: Lung cancer remains one of the leading causes of cancer-related mortality worldwide, necessitating the exploration of novel therapeutic agents. Benzenesulfonamide derivatives have garnered attention for their potential anti-cancer properties.

Objectives: This study aims to investigate the anti-proliferative effects of these compounds on human lung cancer cells and to elucidate the underlying pathways involved in their mechanism of action.

Materials and Methods: In this in-vitro study, we investigated the cytotoxic effects of acetazolamide, a pan inhibitor, along with its parent compound C3 and its derivatives C4 and C6 against A549 lung cancer cells. We evaluated key intracellular parameters including pH levels, reactive oxygen species (ROS) production, and the expression of carbonic anhydrases 9 and 12. To assess cell viability and death, we employed the acridine orange/propidium iodide assay, which allowed us to differentiate between live and dead cells.

Results: The results of this study indicated that the compounds C3, C4, C6, and acetazolamide effectively reduced the proliferation of A549 lung cancer cells after 72 hours of treatment. Notably, C3 was associated with an increase in ROS levels, suggesting a potential mechanism for its cytotoxicity. In contrast, C6 demonstrated a reduction in ROS levels, while C4 exhibited no significant effect on ROS production. All tested compounds were found to decrease intracellular pH, which may contribute to their anti-proliferative effects.

Conclusion: The findings highlight the promising potential of benzenesulfonamide derivatives as effective anti-proliferative agents against A549 lung cancer cells. The diverse mechanisms through which these compounds exert their cytotoxic effects, including modulation of ROS levels and intracellular pH, underscore their multifaceted nature in targeting cancer cell viability.

Citation: Miran HN, Jasim GA, Abidtawfeeq TH. Investigating the anti-proliferative effects of benzenesulfonamide derivatives on human lung cancer cells; an in-vitro analysis study. Immunopathol Persa. 2025;x(x):e43824. DOI:10.34172/ipp.2025.43824.

Introduction

Cancer continues to be a leading cause of death globally, with traditional treatments like surgery, chemotherapy, and radiotherapy often showing limited effectiveness in advanced stages due to the development of resistance to single-agent therapies. To address this challenge, there is a growing emphasis on therapeutic strategies that simultaneously target multiple molecular pathways, which have been associated with significantly better clinical outcomes. Current research is focused on creating therapies that specifically modulate critical cancer signaling pathways, thereby providing more targeted and effective treatment options for patients (1, 2). Tackling drug resistance in cancer therapy, particularly due to the complexities of tumor cell heterogeneity and the protective features of the microenvironment, is now considered attainable through precise pharmacological interventions. Environmental factors drive metabolic changes, such as the "Warburg effect," where cancer cells favor glycolysis over oxidative phosphorylation, even in oxygen-rich conditions, to promote survival and proliferation. These environmental factors, often defined by acidic conditions and low oxygen levels, contribute to the development of highly invasive cancer phenotypes that exhibit resistance to standard treatments and are linked to unfavorable outcomes (3,4).

Proliferating cancerous cells can preserve an optimal intracellular pH despite the surrounding acidity, supporting their survival and proliferation. Hypoxia-inducible factors play a pivotal role in the adaptation to low-oxygen levels by regulating genes that control metabolic processes, pH homeostasis, and angiogenesis, which are crucial for cancer

Key point

The findings of this investigation underscore the significant potential of benzenesulfonamide derivatives as effective anti-proliferative agents against A549 lung cancer cells. These compounds demonstrated a marked ability to inhibit cell proliferation, suggesting that they could serve as promising candidates for the development of novel therapeutic strategies in lung cancer treatment. The promising anti-proliferative effects of benzenesulfonamide derivatives suggest a potential avenue for developing novel therapeutic agents that could enhance current treatment protocols. Policymakers should consider integrating these findings into guidelines for lung cancer management, promoting further research into the clinical applications of these compounds. Additionally, the study emphasizes the importance of understanding cellular mechanisms, which should be incorporated into medical education curricula to better prepare future healthcare professionals. By fostering a deeper understanding of these mechanisms, researchers and clinicians can collaborate more effectively to innovate treatment strategies that improve patient outcomes in lung cancer care.

cells to thrive in hypoxic environments (5). Elevated levels of reactive oxygen species (ROS) in malignant cells, driven by their enhanced metabolic activity, contribute to increased proliferation, genetic instability, and therapeutic resistance, highlighting the dual role of ROS in tumorigenesis and treatment efficacy (6,7). Regulating ROS levels can have opposing effects, either inhibiting or promoting tumor development, making ROS a complex yet promising target for cancer therapy (8). Reducing ROS levels in cancer cells can disrupt their metabolic adaptations, decrease cell proliferation, and limit genetic instability, thereby potentially impeding tumor growth (9). Studies have shown that antioxidants can enhance the efficacy of chemotherapy, alleviate side effects, and protect healthy tissues from damage (10). On the other hand, pushing ROS levels past a toxic limit can lead to cancer cell death by initiating apoptosis or driving the cells into senescence (8). A wide range of chemotherapy drugs promote the generation of ROS within cancer cells, leading to imbalances in cellular homeostasis and resulting in oxidative damage to DNA, proteins, and lipids, which significantly contributes to their ability to induce cell death (11). Excessive ROS generation can boost the pro-apoptotic effects of anticancer drugs and influence cell cycle regulation (12). Therefore, strategically modulating ROS levels, whether by increasing or decreasing them, can effectively harness their dual roles in promoting and inhibiting tumor growth for cancer therapy (8).

Objectives

The objective of this study is to investigate the anti-proliferative effects of benzenesulfonamide derivatives on human lung cancer cells. By employing in-vitro analysis techniques, this research aims to identify the efficacy of various benzenesulfonamide derivatives in inhibiting cell proliferation. Ultimately, the study seeks to contribute to the development of novel therapeutic strategies for lung cancer treatment by providing insights into the potential of these compounds as effective anti-cancer agents.

Materials and Methods

Study design

The in vitro experimental study was conducted at the Pharmacy College of Mustansiriyah University in Baghdad, Iraq, with the primary objective of evaluating the effects of synthesized benzenesulfonamide derivatives on human lung cancer cells, specifically targeting the A549 cell line. This research aimed to explore the anti-proliferative activity of these novel compounds and their potential mechanisms of action, contributing to the understanding of therapeutic strategies against lung cancer. This investigation utilized various assays to assess cell viability and morphological changes in response to treatment.

Cell culture conditions

The A549 cell line was procured from the American type culture collection (ATCC, USA) and cultured in Roswell Park Memorial Institute 1640 medium (RPMI 1640) (Capricorn, Germany), supplemented with 10% fetal bovine serum (FBS) (v/v) and antibiotics including 100 µg/mL streptomycin and 100 IU/mL penicillin (Capricorn, Germany). The cells were maintained in a humidified incubator with a 5% carbon dioxide (CO2) atmosphere at 37 °C, ensuring optimal growth conditions. For experimental assays, only cultures exhibiting over 75% confluence were utilized, allowing for consistent and reliable results in evaluating the effects of treatments on cell viability and morphology (13).

Compounds

The sulfonamide derivatives C4 and C6 were synthesized from the parent compound C3 in Iraq, and their anti-proliferative effects were evaluated through in vitro experiments (14). Stock solutions of the compounds C3, C4, and C6, along with the standard drug acetazolamide (ACZ) sourced from China, were prepared at a concentration of 50 mM using dimethyl sulfoxide (DMSO) as the solvent, which was obtained from India. To facilitate the experimental procedures, the stock solutions were subsequently diluted using either Roswell Park Memorial Institute Medium or Dulbecco's modified eagle medium (Capricorn, Germany).

Assessment of cell viability

The assessment of cell viability was performed using the human adenocarcinoma alveolar epithelial cell line A549, which was originally isolated from the lung tissue of a 58-year-old White male diagnosed with carcinoma (15). The cytotoxicity of the synthesized test compounds was evaluated through the Water-Soluble Tetrazolium/Cell Counting Kit-8 (WST-8/CCK-8) assay, following the manufacturer's guidelines provided by Elabscience®. In this assay, 100 µL of a cell suspension containing 5000 cells were added to each well of a 96-well microplate, along with 100 µL of culture medium in wells designated

as controls (without cells). The cells were treated with various concentrations (31.5, 62.5, 125, 250, 500, and 1000 µM) of the test compounds C3, C4, C6, and the ACZ in RPMI 1640 medium supplemented culture medium and incubated for 72 hours at 37 °C. Following treatment, 10 µL of CCK-8 buffer were added to each well and incubated for an additional 4 hours. The WST-8 reagent is reduced to an orange formazan product by mitochondrial dehydrogenases, and the amount of formazan produced is directly proportional to the number of viable cells. Subsequently, the optical density was assessed at 492 nm using a microplate reader from Gennex Lab (USA) (16), and the half-maximal inhibitory concentration values were determined and presented in dose-response curves using GraphPad Prism version 10.01. This experiment was conducted in triplicate to ensure statistical reliability and accuracy in assessing the anti-proliferative effects of the test compounds on A549 cells.

Fluorometric ROS assay

To evaluate the role of oxidative stress in the cell death induced by the test compounds C3, C4, and C6, a fluorometric ROS assay was conducted using the fluorescent probe 2,7-dichlorofluorescein diacetate (DCFH-DA), sourced from Elabscience® (USA). A549 cells were plated on black microplates and treated with the half-maximal inhibitory concentration (IC50) values of compounds C3, C4, and C6, followed by incubation for 24 hours at 37 °C. After incubation, the cells were harvested and centrifuged at 1000 times the gravitational force (g) for 5 minutes, then rinsed twice with a serum-free medium to remove any residual compounds. The cell pellets were subsequently stained with DCFH-DA at a concentration of 2.5 µM/mL for 30 minutes in the dark at 37 °C. Following staining, ROS levels were quantified using a fluorescence microplate reader with an excitation wavelength of 500 nm and an emission wavelength of 525 nm (17).

Fluorescence intracellular pH assay

The fluorescence intracellular pH assay was conducted using the fluorometric intracellular pH kit (MAK-150) from Sigma Aldrich (USA) to evaluate the levels of pH within the cells. The assay utilized the fluorescent indicator 2',7'-dichlorofluorescein diacetate (BCFL-AM), which is optimized for permeating cellular membranes, allowing for accurate measurement of intracellular pH fluctuations. A549 cells were plated at a density of 40 000 cells per well on a black microplate and incubated for 24 hours at 37 °C. Following incubation, the culture medium was replaced with the BCFL-AM reagent, and the cells were further incubated in a 5% carbon dioxide CO2 atmosphere for 30 minutes while protected from light. Subsequently, the half-maximal IC50 doses of test compounds C3, C4, and C6 were incorporated into the HEPES-buffered saline (HBS) solution. After a 5-minute incubation period, the fluorescence intensity was determined using a spectrofluorimeter at excitation and emission wavelengths of 490 nm and 535 nm, respectively (18).

Bicinchoninic acid protein colorimetric assay

The bicinchoninic acid (BCA) protein colorimetric assay was employed to quantify the total protein content in cell samples, serving as a normalization step for subsequent analyses. To prepare the BCA working solution, 4 µL of copper (II) sulfate solution were mixed with 196 µL of BCA reagent for each well, resulting in a final volume of 200 µL per well. Concurrently, a standard protein solution was prepared at a concentration of one milligram per milliliter (mg/mL) by dissolving a standard vial in 1 milliliter of standard diluent and mixing thoroughly. For the generation of a standard curve, fresh standards were prepared each time by diluting the one mg/mL standard solution in standard diluent to create a series of concentrations ranging from 0 to one mg/mL; these standard dilutions were used once and subsequently discarded. The standard curve for the BCA assay is illustrated in (Figure 1). In parallel, cell preparation involved harvesting 1×10^6 A549 cells per assay, which were washed with phosphate-buffered saline (PBS) and homogenized. The homogenates were then centrifuged at 10 000 times the gravitational force (g) for 10 minutes at 4 °C to remove insoluble material, and the supernatant was collected and kept on ice for detection. The optical density values of each well were measured at 562 nm using a microplate reader, allowing for accurate quantification of protein content in the samples.

Enzyme-linked immunosorbent assay of carbonic anhydrase XII (CA-12)

The human enzyme-linked immunosorbent assay (ELISA) for CA-12 was performed following the manufacturer's protocol provided by RayBio® (USA). Initially, samples and reagents were equilibrated to room temperature (18 - 25 °C). A total of 100 µL of each standard and sample, which consisted of cell culture media from the A549 cancer cell line treated with compounds C3, C4, and C6, were added to the designated wells after a 24-hour incubation period. The wells were covered and incubated at room temperature for 2.5 hours with mild agitation. After incubation, the solution was removed, and the wells were rinsed four times with wash solution (1X) using 300 µL per well, followed by flipping the plate to absorb excess liquid on clean paper towels. Subsequently, 100 µL of biotinylated antibody (1X) were added to each well and incubated at room temperature for 1 hour with gentle agitation. Following this step, the solution was expelled, and the washing procedure was repeated. Then, 100 µL per well of streptavidin solution were added, and the plate was incubated at room temperature for an additional 45 minutes with mild agitation. After removing the solution and repeating the wash phase, 100 µL per well of tetramethyl benzidine (TMB) One-Step substrate reagent were added and incubated in the dark for 30 minutes at

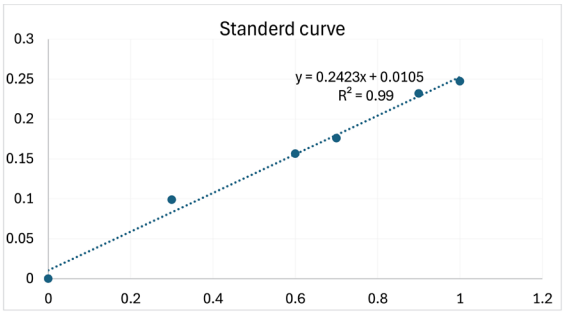

Figure 1. Bicinchoninic acid standard curve.

room temperature with gentle shaking. Finally, 50 µL per well of stop solution were added, and the absorbance was measured immediately at a wavelength of 450 nm (19). The standard curve for CA-12 is illustrated in Figure 2, providing a quantitative assessment of CA-12 levels in the treated samples.

ELISA of carbonic anhydrase IX (CA-9)

The Human CA-9 (Elabscience®) ELISA assay was conducted following a systematic protocol designed for accurate quantification of CA-9 levels. Initially, cells were gently washed with PBS at room temperature, followed by dissociation using trypsin. The resulting cell suspension underwent centrifugation for 5 minutes, after which the medium was discarded, and the cells were rinsed three times with PBS to remove residual trypsin. To preserve the cells, 250 µL of PBS per 1×10^6 cells were added, and cell lysate was obtained through a freeze-thaw technique. The suspension was then centrifuged at 1500×g for 10 minutes at a temperature range of 2-8 °C to separate cell fragments from the supernatant, which was subsequently collected for the assay (19). A standard curve for CA-9 was established, as illustrated in Figure 3, facilitating the quantitative analysis of CA-9 in the samples processed.

Acridine orange/propidium iodide staining assay

The AO/PI (acridine orange/propidium iodide) staining assay was employed to assess apoptotic changes in the A549 cell line, both in control and treated groups (20). Initially, 5000 cells per well were seeded into an 8-well plate and treated with compounds C3, C4, and C6, followed by a 24-hour incubation at 37 °C. After treatment, a stain mixture of AO/PI was added at 50 µL per well, which was discarded after 30 seconds to minimize background fluorescence. The morphological changes indicative of apoptosis was then examined using Leica fluorescent microscopy. This method allows for the differentiation between viable, apoptotic, and necrotic cells based on their staining properties, providing valuable insights into the effects of the tested compounds on A549 cell viability and apoptosis induction.

Statistical analysis

Statistical analysis was conducted using one-way and two-

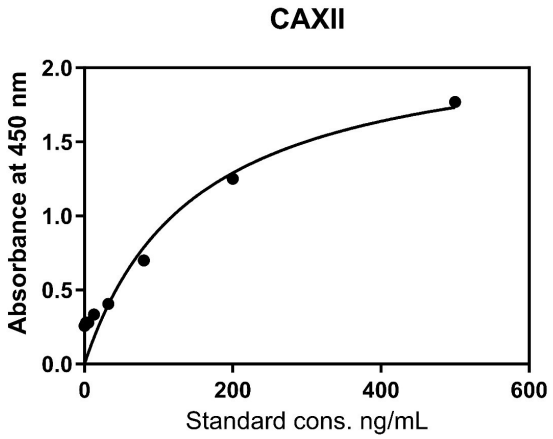

Figure 2. ELISA standard curve of CA-12 for A549 cell line.

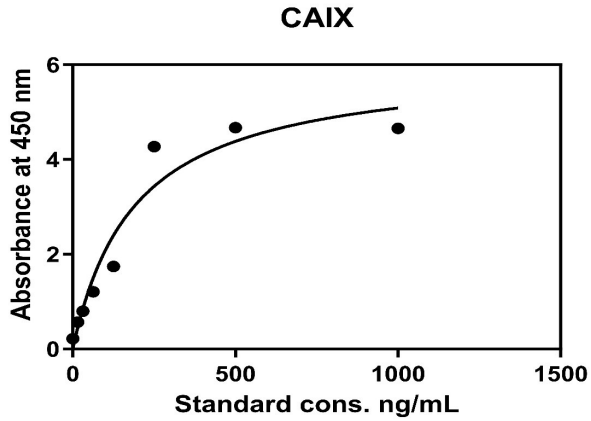

Figure 3. ELISA standard curve of CAIX for A549 cell lines.

way analysis of variance (ANOVA), followed by post-hoc comparisons to evaluate the differences among groups in the in vitro study. The data were expressed as mean ± standard deviation (SD) to represent variability within the datasets. GraphPad Prism version 10.01 for Windows was utilized for all statistical computations. A p-value of less than 0.05 was considered statistically significant, with specific thresholds: $*P<0.05$, $**P<0.001$, $***P=0.0001$, and $****P<0.0001$.

Results

The anti-proliferative activity of compounds C3, C4, C6, and the reference pan inhibitor ACZ was assessed in vitro against the human cancer cell line A549 using the WST-8 colorimetric assay. The results demonstrated that all tested compounds effectively reduced cell proliferation after a 72-hour incubation period, exhibiting a dose-dependent decrease in cytotoxicity; higher concentrations of each compound correlated with increased cytotoxic effects (Figure 4).

The dose-response curves for determining the IC50 value of four test compounds on A549 cancer cells were obtained by WST-8 assay after 72 hours of cell culture. The x-axis represents the logarithm concentration of the

test compounds (in µg), and the y-axis represents the percentage of normalized absorbance. The IC50 value, represented by the Log of drug concentration of the test compounds inhibits 50% of cell viability. The dose-response curves revealed that acetazolamide exhibited the highest potency with an IC50 value of 68.8 µg/mL. In comparison, compound C3 displayed moderate cytotoxicity with an IC50 of 171.2 µg/mL, while compound C4 showed slightly lower potency with an IC50 of 213.7 µg/mL; compound C6 had an IC50 value of 160.1 µg/mL. These IC50 values provide a quantitative measure of the dose-dependent effects of the compounds on A549 cells, highlighting their varying levels of cytotoxicity (Figure 5).

Cell morphology analysis of the A549 cell line, assessed through the WST assay, revealed significant alterations indicative of cytotoxicity, including cell shrinkage, membrane protrusions, and the formation of apoptotic bodies. These morphological changes are characteristic of apoptotic processes and suggest a progression toward cell death in response to treatment. Additionally, observations of cell density indicated a marked reduction in the density of treated cells compared to the control group, further supporting the conclusion that the compounds exert cytotoxic effects on the A549 lung cancer cells (Figure 6).

In the comparative analysis of the ROS level in cancer cells treated with studied compounds, Figure 7 presents a bar graph illustrating the levels of ROS in A549 cell lines across four distinct groups: control (untreated cells), C3,

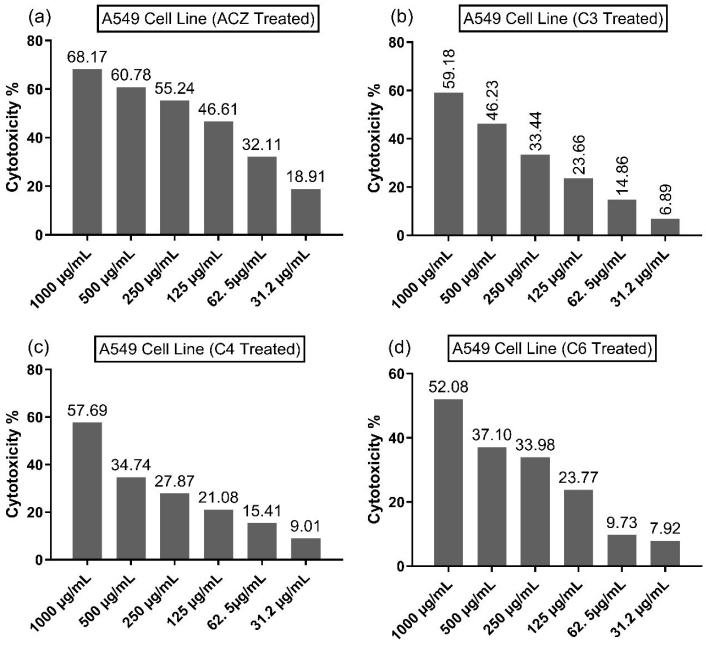

Figure 4. Cytotoxic effect of varying concentrations of four test compounds obtained by WST-8 assays after 72 h of culture for lung cancer cell line A549

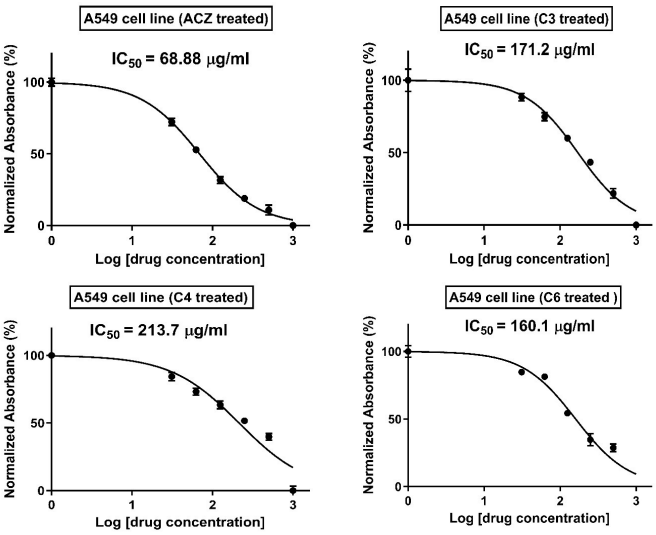

Figure 5. The dose-response curve for determining the IC50 value of four test compounds on A549 cancer cells obtained by WST-8 assay after 72 h of cell culture.

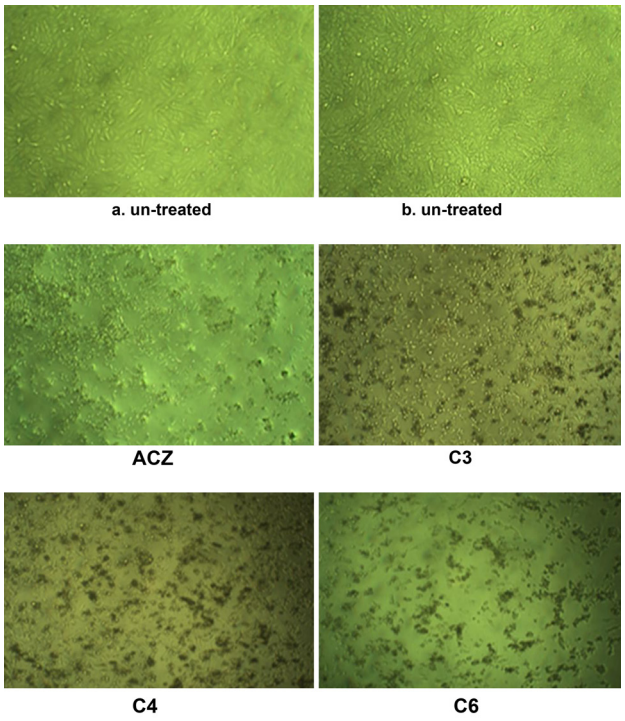

Figure 6. Morphological changes in A549 lung cancer cells observed by WST assay after 72 hours of treatment with ACZ, C3, C4, and C6 compounds under the inverted microscope.

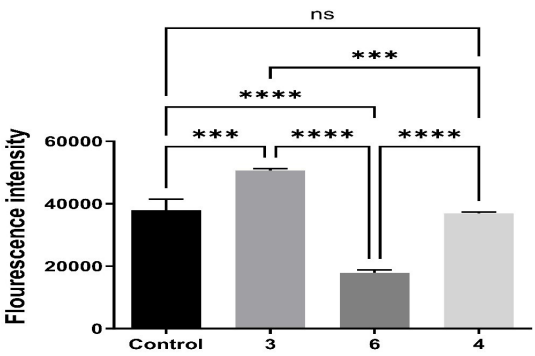

Figure 7. Alterations in ROS levels in A549 cancer cells measured by fluorescence microplate reader following DCFDA staining.

C6, and C4. The X-axis categorizes these groups, while the Y-axis indicates fluorescence intensity, which serves as a proxy for the amount of ROS generated within the cells. Notably, the C3-treated group exhibited a significantly elevated ROS level compared to the control group, with this increase reaching statistical significance. Conversely, the C6 compound demonstrated a significant reduction in ROS levels relative to the control. In contrast, the comparison between the control and C4 compound revealed only a small mean difference that was not statistically significant. Furthermore, a comparison between the C3 and C6 compounds indicated a substantial difference, underscoring a strong statistical significance in ROS generation between these two treatment groups (Table 1 and Figure 7).

The bar graph illustrates the effects of the compounds C3, C4, and C6 on intracellular pH levels in the A549 cell line, as indicated by fluorescence intensity. The control group served as a reference for normal intracellular pH, revealing that treatments with C3, C4, and C6 resulted in varying degrees of pH reduction. Notably, the C3 compound significantly decreased intracellular pH compared to the control, as evidenced by a marked reduction in fluorescence intensity. Similarly, the C6 compound also induced a significant reduction in intracellular pH levels relative to the control. Furthermore, the C4 compound demonstrated a statistically significant decrease in fluorescence intensity, indicating its impact on lowering intracellular pH as well (Table 2 and Figure 8).

Figure 9 presents the concentrations of CA-12 and CA-9 across different treatments in the A549 lung cancer cell line. The CA-12 concentrations exhibited minimal variation among the control, C3, and C6 compounds, with a significant increase noted only in the C4-treated cells. This suggests that the treatments exert minimal differential effects on CA-12 levels in A549 cells. Similarly, the concentrations of CA-9 remained relatively consistent across the control, C3, C4, and C6 treatments. The lack of significant variation in CA-9 levels indicates that these compounds do not have substantial effects on CA-9 concentrations in A549 cells (Table 3 and Figure 9).

Figure 10 presents a bar graph illustrating cell death resulting from DNA damage in viable and dead A549 cells, as indicated by fluorescence intensity under various treatments. The analysis revealed that the C3, C4, and C6 compounds significantly increased the number of dead cells compared to the control group across all treatments. In the control group, the difference in DNA damage between viable and dead cells was highly significant,

Table 1. Comparison of the ROS level in cancer cells treated with C3, C4, and C6 compounds using Tukey's multiple comparisons test

Compound	Mean difference	95% CI	Below threshold?	Summary	*P* value*
Control versus C3	-12737	-17998 to -7477	Yes	***	0.0004
Control versus C6	20031	14771 to 25292	Yes	****	<0.0001
Control versus C4	1124	-4758 to 7005	No	ns	0.9183
C3 versus C6	32769	27508 to 38029	Yes	****	<0.0001
C3 versus C4	13861	7980 to 19742	Yes	***	0.0005
C6 versus C4	-18908	-24789 to -13026	Yes	****	<0.0001

* ANOVA followed by the post hoc LSD test; ns, Non-significant; CI, Confidence interval.

Table 2. CTukey's multiple comparisons test of pH assay for A549 between four groups of C3, C4, C6, and control

Compound	Mean difference	95% CI	Below threshold?	Summary	*P* value*
C3 versus C4	-685.6	-3470 to 2099	No	ns	0.8938
C3 versus C6	-879.4	-3664 to 1905	No	ns	0.8031
C3 versus Control	-4185	-6970 to -1401	Yes	**	0.0028
C4 versus C6	-193.8	-2978 to 2591	No	ns	0.9971
C4 versus Control	-3500	-6284 to -715.3	Yes	*	0.0116
C6 versus Control	-3306	-6090 to -521.5	Yes	*	0.0174

* ANOVA followed by the post hoc LSD test; ns, Non-significant; CI, Confidence interval.

highlighting the impact of treatment on cellular integrity. Furthermore, among the viable cells, exposure to the C3, C4, and C6 compounds resulted in a significant reduction in cell viability compared to the control group, as supported by additional presented data (Table 4 and Figure 10); and morphological alterations (Figure 11).

Discussion

The findings of this study revealed that compounds C3, C4, C6, and acetazolamide significantly inhibited the proliferation of A549 lung cancer cells. The C3 was significantly correlated to an increase in ROS levels, indicating a possible mechanism for its cytotoxic effects. In contrast, C6 resulted in decreased ROS levels, while C4 had no substantial impact on ROS production. All compounds tested were observed to reduce intracellular pH, which may contribute to their anti-proliferative properties.

This finding that C3 significantly elevates ROS levels suggests a pro-oxidant effect, which may contribute to the promotion of apoptosis and cytotoxicity. This finding is consistent with the research conducted by Sies and Jones (21), which also highlights the role of increased ROS in cellular processes leading to programmed cell death and toxicity. Such alignment between the current findings and previous studies underscores the importance of ROS as a critical mediator in the context of C3's biological effects. In contrast, the result that C6 significantly decreased ROS levels, indicating its potential antioxidant properties, aligns with the findings of Leporini et al (22), this correlation underscores the role of C6 as a promising agent in mitigating oxidative stress, thereby supporting the hypothesis that compounds exhibiting antioxidant activity can effectively lower ROS levels. Such results contribute to a growing body of literature that emphasizes the importance of exploring antioxidant mechanisms in various therapeutic contexts, highlighting C6's relevance in future research aimed at understanding its protective effects against oxidative damage. Conversely, C4 demonstrated no significant impact on ROS levels in A549 cells, suggesting that its mechanism of action may be independent of oxidative stress pathways. A549 cells, originating from lung carcinoma, are characterized by a mixed metabolic phenotype that often exhibits a pronounced glycolytic component, particularly under specific environmental conditions (23). This lack of effect on ROS indicates that C4 may exert its influence through alternative biological mechanisms, warranting further investigation into its metabolic interactions and potential therapeutic applications in cancer treatment.

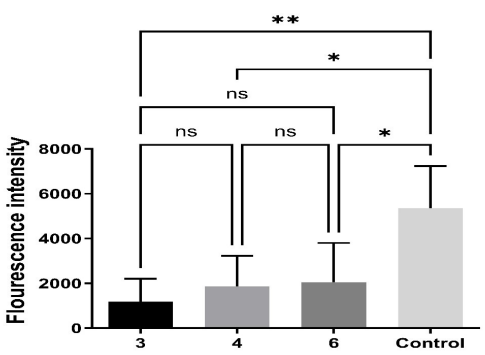

Figure 8. Effects of compounds C3, C4, and C6 on intracellular pH levels in A549 cancer cells as measured by fluorescence intensity assay.

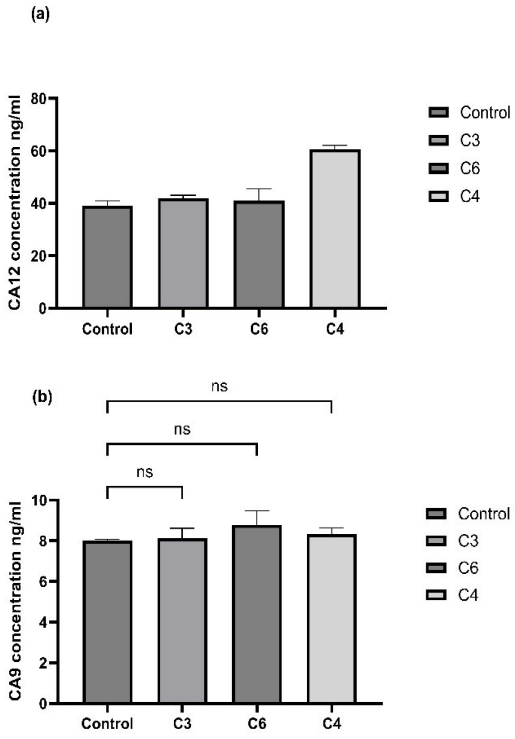

Figure 9. Effects of compounds C3, C4, and C6 on CA-12 (a) and CA-9 (b) in A549 cancer cells.

Table 3. Comparison of the CA-12 and CA-9 in cancer cells between compounds of C3, C4, and C6

Compound		Mean difference	95% CI	Below threshold?	Summary	*P* value*
CA-12(ng/mL)	Control versus C3	-2.938	-13.57 to 7.690	No	ns	0.6958
	Control versus C6	-1.961	-12.59 to 8.667	No	ns	0.8723
	Control versus C4	-21.5	-32.13 to -10.87	Yes	**	0.0041
	C3 versus C6	-0.9774	-9.651 to 11.61	No	ns	0.9798
	C3 versus C4	-18.56	-29.19 to -7.932	Yes	*	0.0071
	C6 versus C4	-19.54	-30.17 to -8.910	Yes	*	0.0059
CA-9 (ng/mL)	Control versus C3	-0.1207	-1.951 to 1.710	No	ns	0.9922
	Control versus C6	-0.7756	-2.606 to 1.055	No	ns	0.4182
	Control versus C4	-0.3093	-2.140 to 1.055	No	ns	0.8969
	C3 versus C6	-0.655	-2.486 to 1.521	No	ns	0.5331
	C3 versus C4	-0.1887	-2.019 to 1.642	No	ns	0.9721
	C6 versus C4	0.4663	-1.364 to 2.297	No	ns	0.7403

* ANOVA followed by the post hoc LSD test; ns, Non-significant; CI, Confidence interval.

Table 4. Comparisons of AO/PI assay for A549 using Šídák›s multiple comparisons test

Compound		Mean difference	95% CI	Below threshold?	Summary	*P* value*
C3 (Viable versus Dead)		-26.14	-32.21 to -20.07	Yes	****	<0.0001
C4 (Viable versus Dead)		-35.17	-41.24 to -29.11	Yes	****	<0.0001
C6 (Viable versus Dead)		-7.687	-13.75 to -1.621	Yes	*	0.0162
Control (Viable versus Dead)		96.75	90.68 to 102.8	Yes	****	<0.0001
Viable	C3 versus C4	4.517	-4.062 to 13.10	No	ns	0.5783
	C3 versus C6	-9.227	-17.81 to -0.6277	Yes	*	0.0314
	C3 versus Control	-61.44	-70.02 to -52.86	Yes	****	<0.0001
	C4 versus C6	-13.74	-22.32 to -5.164	Yes	**	0.0012
	C4 versus Control	-65.96	-74.54 to -57.38	Yes	****	<0.0001
	C6 versus Control	-52.22	-60.80 to -43.64	Yes	****	<0.0001
Dead	C3 versus C4	-4.517	-13.10 to 4.062	No	ns	0.5783
	C3 versus C6	9.227	0.6477 to 17.81	Yes	*	0.0314
	C3 versus Control	61.44	52.86 to 70.02	Yes	****	<0.0001
	C4 versus C6	13.74	5.164 to 22.32	Yes	**	0.0012
	C4 versus Control	65.96	57.38 to 74.54	Yes	****	<0.0001
	C6 versus Control	52.22	43.64 to 60.80	Yes	****	<0.0001

* ANOVA followed by the post hoc LSD test; ns, Non-significant; CI, Confidence interval.

Understanding the metabolic characteristics of A549 cells is crucial for elucidating the broader implications of C4's action within the context of lung cancer biology.

In our study, we observed that all tested compounds significantly reduced intracellular pH, a finding that may play a crucial role in their anti-proliferative properties. An alkaline intracellular pH is crucial for cancer cells as it facilitates their metabolic activities, particularly glycolysis. Disruptions in pH regulation can lead to metabolic disturbances and impaired mitochondrial function, which in turn elevate ROS production. Such pH imbalances may induce metabolic stress and compromise energy production efficiency, compelling mitochondria to exert greater effort to fulfill energy requirements, resulting in increased electron leakage and subsequent ROS generation. Moreover, if cells transition towards enhanced oxidative phosphorylation under altered conditions, the mitochondria may struggle to meet the heightened energy demands, exacerbating ROS output. Additionally, fluctuations in pH can adversely affect the functionality of antioxidant enzymes, diminishing the cells' ability to scavenge ROS effectively and consequently elevating overall ROS levels. This interplay between pH regulation and mitochondrial dynamics underscores the significance of maintaining optimal intracellular conditions for cellular health and function in cancer biology (24,25). The reduction in intracellular pH can induce metabolic alterations that hinder cancer cell proliferation, as many cancer cells rely on a tightly regulated pH environment to support their growth and metabolic activities. By decreasing pH levels, these compounds may disrupt the cellular mechanisms that facilitate energy production and biosynthesis, thereby impairing the cancer cells' ability to proliferate effectively. This suggests that the modulation of intracellular pH could be a strategic approach in developing therapeutic agents aimed at inhibiting tumor growth, highlighting the need for further investigation into the underlying mechanisms through which these compounds exert their effects on cellular metabolism and proliferation.

The observed effects of compounds C3, C4, and C6 on carbonic anhydrase isoforms CA-12 and CA-9 in

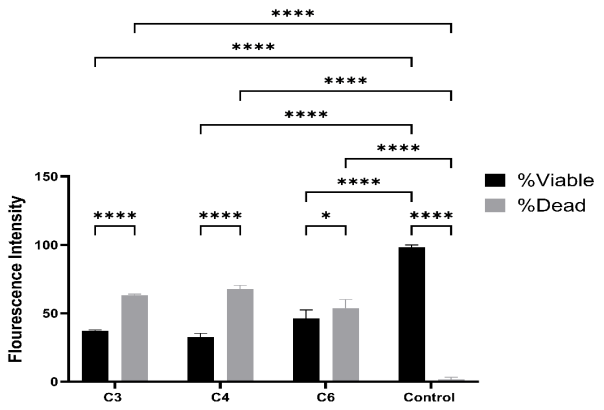

Figure 10. Illustrated results obtained by using AO/PI assay on A549 cancer cells.

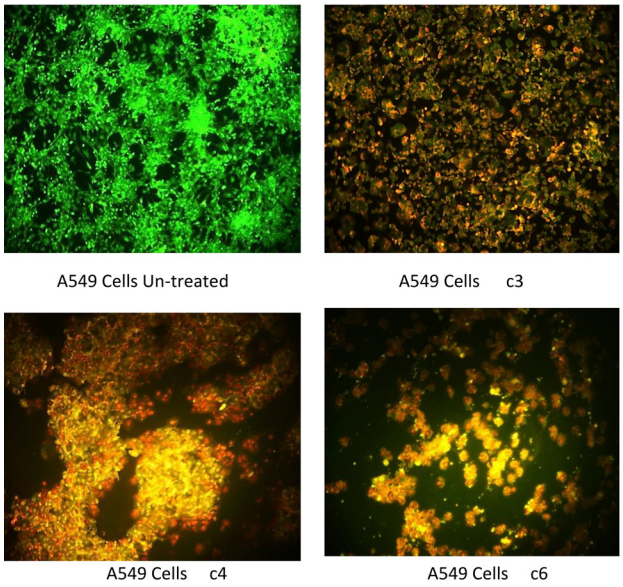

Figure 11. Morphological alteration in the A549 cell line in compounds of C3, C4, C6, and untreated cells

the A549 cell line indicate that these compounds may exert their actions through distinct mechanisms that are influenced by the specific cellular context. This study highlights the intricate regulation of carbonic anhydrase in cancer cells, aligning with previous research that emphasizes the significant role of cell-specific factors and the compensatory strategies that emerge in response to pH disruption (26). Notably, the up-regulation of CA-12 levels in C4-treated cells suggests a potential compensatory mechanism aimed at counteracting the effects of altered pH (27, 28). Furthermore, the results from the intracellular pH assay demonstrated that compounds C3, C4, and C6 effectively reduced intracellular pH, indicating that their actions may involve mechanisms independent of carbonic anhydrases CA-12 and CA-9 in A549 cells (29,30). The differential modulation of these enzymes suggests that each compound interacts with the cellular environment in unique ways, potentially affecting metabolic pathways and regulatory networks associated with tumor growth and progression. This variability highlights the importance of considering the cellular microenvironment when evaluating the pharmacological effects of these compounds, as their efficacy may be contingent upon the presence of specific cellular factors or conditions. Further elucidation of these mechanisms could provide valuable insights into the therapeutic potential of C3, C4, and C6 in targeting carbonic anhydrases within lung cancer cells, ultimately contributing to more effective treatment strategies. This finding underscores the necessity of further investigating the interplay between pH regulation and carbonic anhydrase activity, as well as the broader implications for therapeutic interventions targeting metabolic pathways in lung cancer.

The results of the AO/PI assay revealed significant cytotoxic effects of the test compounds C3, C4, and C6 on A549 cells, demonstrating varying degrees of efficacy in reducing cell viability and inducing cell death. All three compounds markedly decreased cell viability compared to the control group, with C4 exhibiting the highest potency, followed closely by C3. Both C3 and C4 displayed strong anti-proliferative effects, while C6 showed a comparatively lesser impact. These findings suggest that the mechanisms underlying the cytotoxicity of these compounds may differ, potentially influenced by their structural properties or interactions within the cellular environment. The pronounced efficacy of C4 and C3 indicates their potential as therapeutic agents in targeting lung cancer cells, warranting further investigation into their specific pathways of action and long-term effects on cellular function. This study contributes to the understanding of how these compounds can selectively induce apoptosis in cancer cells, highlighting their relevance in the development of novel anticancer therapies. The differential cytotoxic effects observed among C3, C4, and C6 suggest that specific structural features or mechanisms may enhance their ability to target cancer cells effectively. The pronounced potency of C4 raises questions about its potential as a lead compound for further development, particularly in optimizing its formulation for clinical use. Additionally, understanding the pathways through which these compounds induce cell death could provide insights into overcoming resistance mechanisms commonly encountered in cancer therapies.

Conclusion

In conclusion, this study demonstrates that benzenesulfonamide derivatives, specifically C3, C4, C6, and acetazolamide, exhibit significant anti-proliferative effects on A549 lung cancer cells through various mechanisms. The observed increase in ROS levels with C3 suggests a potential pathway for inducing cytotoxicity, while C6's ability to reduce ROS levels indicates a distinct mechanism that may also contribute to its efficacy. All compounds effectively lowered intracellular pH, further

supporting their role in inhibiting cell proliferation. These findings underscore the potential of benzenesulfonamide derivatives as novel therapeutic agents in lung cancer treatment and warrant further investigation into their mechanisms of action and clinical applicability. Future research should focus on elucidating the specific molecular pathways involved and exploring the clinical applicability of these compounds to enhance treatment outcomes for lung cancer patients.

Limitations of the study

Several limitations were identified in this study investigating the anti-proliferative effects of benzenesulfonamide derivatives on human lung cancer cells. Firstly, the research was conducted solely in vitro using A549 lung cancer cell lines, which may not fully replicate the complex tumor microenvironment and heterogeneity observed in vivo. Consequently, the results may not accurately predict the efficacy of these compounds in clinical settings. Secondly, while the study evaluated key intracellular parameters such as ROS and pH levels, it did not explore other potential mechanisms of action or signaling pathways that could contribute to the observed anti-cancer effects. Furthermore, the duration of treatment (72 hours) may not be sufficient to capture long-term effects or resistance mechanisms that could develop with prolonged exposure to these compounds. Lastly, potential off-target effects and toxicity profiles of benzenesulfonamide derivatives were not assessed, which is crucial for evaluating their therapeutic viability.

Acknowledgments

The authors would like to express their sincere gratitude to the Pharmaceutical Chemistry Department at the College of Pharmacy, University of Mustansiriyah, Iraq, for their invaluable support and assistance throughout this research.

Authors' contribution

Conceptualization: Hiba Nabil Miran.
Data curation: Hiba Nabil Miran and Ghaith Ali Jasim.
Formal analysis: Ghaith Ali Jasim.
Investigation: Tareq Hafdhi Abidtafq and Ghaith Ali Jasim.
Methodology: Ghaith Ali Jasim.
Project administration: Hiba Nabil Miran.
Resources: All authors.
Software: Ghaith Ali Jasim.
Supervision: Tareq Hafdhi Abidtafq.
Validation: Tareq Hafdhi Abidtafq.
Visualization: Hiba Nabil Miran and Tareq Hafdhi Abidtafq.
Writing–original draft: All authors.
Writing–review & editing: All authors.

Conflicts of interest

The authors declare no conflict of interest.

Ethical issues

The research was conducted in accordance with the tenets of the Declaration of Helsinki. The research protocol for this study received approval from the Ethics Committee of the University of Mustansiriyah, Pharmacy College, Iraq, which ensuring compliance with ethical standards in research practices (Ethical code #6871/21). The authors have diligently adhered to ethical considerations throughout the study, including the avoidance of plagiarism, data fabrication, and double publication.

Funding/Support

The authors did not receive any source of funding.

References

1. Abbas HS, Nossier ES, El-Manawaty MA, El-Bayaa MN. New sulfonamide-based glycosides incorporated 1,2,3-triazole as cytotoxic agents through VEGFR-2 and carbonic anhydrase inhibitory activity. Sci Rep. 2024;14:13028. doi: 10.1038/s41598-024-62864-9.
2. Liu Q, Yu S, Zhao W, Qin S, Chu Q, Wu K. EGFR-TKIs resistance via EGFR-independent signaling pathways. Mol Cancer. 2018;17:53. doi: 10.1186/s12943-018-0793-1.
3. Roma-Rodrigues C, Mendes R, Baptista PV, Fernandes AR. Targeting Tumor Microenvironment for Cancer Therapy. Int J Mol Sci. 2019;20. doi: 10.3390/ijms20040840.
4. Schwartz L, Supuran CT, Alfarouk KO. The Warburg Effect and the Hallmarks of Cancer. Anticancer Agents Med Chem. 2017;17:164-70. doi: 10.2174/1871520616666161031143301.
5. Liao R, Ma QZ, Zhou CY, Li JJ, Weng NN, Yang Y, et al. Identification of biomarkers related to Tumor-Infiltrating Lymphocytes (TILs) infiltration with gene co-expression network in colorectal cancer. Bioengineered. 2021;12:1676-88. doi: 10.1080/21655979.2021.1921551.
6. Pelicano H, Carney D, Huang P. ROS stress in cancer cells and therapeutic implications. Drug Resist Updat. 2004;7:97-110. doi: 10.1016/j.drup.2004.01.004.
7. Marinho HS, Real C, Cyrne L, Soares H, Antunes F. Hydrogen peroxide sensing, signaling and regulation of transcription factors. Redox Biol. 2014;2:535-62. doi: 10.1016/j.redox.2014.02.006.
8. Sahoo BM, Banik BK, Borah P, Jain A. Reactive Oxygen Species (ROS): Key Components in Cancer Therapies. Anticancer Agents Med Chem. 2022;22:215-22. doi: 10.2174/1871520621666210608095512.
9. Moloney JN, Cotter TG. ROS signalling in the biology of cancer. Semin Cell Dev Biol. 2018;80:50-64. doi: 10.1016/j.semcdb.2017.05.023.
10. Prieto-Bermejo R, Romo-González M, Pérez-Fernández A, Ijurko C, Hernández-Hernández Á. Reactive oxygen species in haematopoiesis: leukaemic cells take a walk on the wild side. J Exp Clin Cancer Res. 2018;37:125. doi: 10.1186/s13046-018-0797-0.
11. Ling T, Lang WH, Craig J, Potts MB, Budhraja A, Opferman J, et al. Studies of Jatrogossone A as a Reactive Oxygen Species Inducer in Cancer Cellular Models. J Nat Prod. 2019;82:1301-11. doi: 10.1021/acs.jnatprod.8b01087.
12. Srinivas US, Tan BWQ, Vellayappan BA, Jeyasekharan AD. ROS and the DNA damage response in cancer. Redox Biol. 2019;25:101084. doi: 10.1016/j.redox.2018.101084.
13. Maciel LLF, Silva MB, Moreira RO, Cardoso AP, Fernandes C, Horn A, Jr., et al. In Vitro and In Vivo Relevant Antineoplastic Activity of Platinum(II) Complexes toward Triple-Negative MDA-MB-231 Breast Cancer Cell Line. Pharmaceutics. 2022;14: 2013. doi: 10.3390/pharmaceutics14102013.
14. Jasim ST, Mahdi MF. Molecular Modeling, Synthesis, and preliminary pharmacological evaluation of New Sulfonamide Derivatives as Selective Carbonic Anhydrase XII and IX inhibitors. Al-Mustansiriyah J Pharma Sci. 2024;24:137-49. doi: 10.32947/ajps.v24i2.1055.
15. Giard DJ, Aaronson SA, Todaro GJ, Arnstein P, Kersey JH, Dosik H, et al. In vitro cultivation of human tumors: establishment of

cell lines derived from a series of solid tumors. J Natl Cancer Inst. 1973;51:1417-23. doi: 10.1093/jnci/51.5.1417.
16. Sun Y, Zhao J, Ji Z. Bifunctional Platinum(II) Complexes with Bisphosphonates Substituted Diamine Derivatives: Synthesis and In vitro Cytotoxicity. Chem Biodivers. 2017;14. doi: 10.1002/cbdv.201700348.
17. Nensat C, Songjang W, Tohtong R, Suthiphongchai T, Phimsen S, Rattanasinganchan P, et al. Porcine placenta extract improves high-glucose-induced angiogenesis impairment. BMC Complement Med Ther. 2021;21:66. doi: 10.1186/s12906-021-03243-z.
18. Jia Y, Chen L, Chi D, Cong D, Zhou P, Jin J, et al. Photodynamic therapy combined with temozolomide inhibits C6 glioma migration and invasion and promotes mitochondrial-associated apoptosis by inhibiting sodium-hydrogen exchanger isoform 1. Photodiagnosis Photodyn Ther. 2019;26:405-12. doi: 10.1016/j.pdpdt.2019.05.007.
19. Yu WX, Lu C, Wang B, Ren XY, Xu K. Effects of rapamycin on osteosarcoma cell proliferation and apoptosis by inducing autophagy. Eur Rev Med Pharmacol Sci. 2020;24:915-21. doi: 10.26355/eurrev_202001_20076.
20. Ude A, Afi-Leslie K, Okeke K, Ogbodo E. Trypan Blue Exclusion Assay, Neutral Red, Acridine Orange and Propidium Iodide: IntechOpen; 2022. doi: 10.5772/intechopen.105699.
21. Sies H, Jones DP. Reactive oxygen species (ROS) as pleiotropic physiological signalling agents. Nat Rev Mol Cell Biol. 2020;21:363-83. doi: 10.1038/s41580-020-0230-3.
22. Leporini M, Catinella G, Bruno M, Falco T, Tundis R, Loizzo MR. Investigating the Antiproliferative and Antioxidant Properties of Pancratium maritimum L. (Amaryllidaceae) Stems, Flowers, Bulbs, and Fruits Extracts. Evid Based Complement Alternat Med. 2018;2018:9301247. doi: 10.1155/2018/9301247.
23. Prusinkiewicz MA, Tu J, Dodge MJ, MacNeil KM, Radko-Juettner S, Fonseca GJ, et al. Differential Effects of Human Adenovirus E1A Protein Isoforms on Aerobic Glycolysis in A549 Human Lung Epithelial Cells. Viruses. 2020;12:610. doi: 10.3390/v12060610.
24. Louie MC, Ton J, Brady ML, Le DT, Mar JN, Lerner CA, et al. Total cellular ATP production changes with primary substrate in MCF7 breast cancer cells. Front Oncol. 2020;10:1703. doi: 10.3389/fonc.2020.01703.
25. Pickles S, Vigié P, Youle RJ. Mitophagy and Quality Control Mechanisms in Mitochondrial Maintenance. Curr Biol. 2018;28:R170-r85. doi: 10.1016/j.cub.2018.01.004.
26. Haapasalo J, Nordfors K, Haapasalo H, Parkkila S. The Expression of Carbonic Anhydrases II, IX and XII in Brain Tumors. Cancers (Basel). 2020;12:1723. doi: 10.3390/cancers12071723.
27. Leppilampi M, Karttunen TJ, Kivelä J, Gut MO, Pastoreková S, Pastorek J, et al. Gastric pit cell hyperplasia and glandular atrophy in carbonic anhydrase IX knockout mice: studies on two strains C57/BL6 and BALB/C. Transgenic Res. 2005;14:655-63. doi: 10.1007/s11248-005-7215-z.
28. Gut MO, Parkkila S, Vernerová Z, Rohde E, Závada J, Höcker M, et al. Gastric hyperplasia in mice with targeted disruption of the carbonic anhydrase gene Car9. Gastroenterology. 2002;123:1889-903. doi: 10.1053/gast.2002.37052.
29. Semenza GL. Pharmacologic Targeting of Hypoxia-Inducible Factors. Annu Rev Pharmacol Toxicol. 2019;59:379-403. doi: 10.1146/annurev-pharmtox-010818-021637.
30. Kaelin WG, Jr. The VHL Tumor Suppressor Gene: Insights into Oxygen Sensing and Cancer. Trans Am Clin Climatol Assoc. 2017;128:298-307.